

# Hybrid Tracker with Pixel and Instance for Video Panoptic Segmentation

Weicai Ye\*, Xinyue Lan\*, Ge Su, Hujun Bao, Zhaopeng Cui and Guofeng Zhang

**Abstract**—Video Panoptic Segmentation (VPS) aims to generate coherent panoptic segmentation and track the identities of all pixels across video frames. Existing methods predominantly utilize the trained instance embedding to keep the consistency of panoptic segmentation. However, they inevitably struggle to cope with the challenges of small objects, similar appearance but inconsistent identities, occlusion, and strong instance contour deformations. To address these problems, we present HybridTracker, a lightweight and joint tracking model attempting to eliminate the limitations of the single tracker. HybridTracker performs pixel tracker and instance tracker in parallel to obtain the association matrices, which are fused into a matching matrix. In the instance tracker, we design a differentiable matching layer, ensuring the stability of inter-frame matching. In the pixel tracker, we compute the dice coefficient of the same instance of different frames given the estimated optical flow, forming the Intersection Over Union (IoU) matrix. We additionally propose mutual check and temporal consistency constraints during inference to settle the occlusion and contour deformation challenges. Comprehensive experiments show that HybridTracker achieves superior performance than state-of-the-art methods on Cityscapes-VPS and VIPER datasets.

**Index Terms**—Video Panoptic Segmentation, Hybrid Tracker, Pixel Tracker, Instance Tracker

## I. INTRODUCTION

VIDEO panoptic segmentation (VPS) aims to assign semantic classes and generate consistent association of instance IDs across video frames with many applications ranging from scene understanding in autonomous driving, video surveillance in smart cities, video editing in entertainment manipulation, etc. Existing methods tackling the problem generally perform the image panoptic segmentation and obtain the matching relationship between adjacent images by calculating the similarity of the instance embedding.

A pioneer work, proposed by [1], first formally defined a brand new task of video panoptic segmentation with a new re-organized dataset and presented a network, i.e., VPSNet, to solve this problem. VPSNet extends UPSNet [2] and adds the MaskTrack head [3] to track each instance, which can track larger objects robustly. However, some small objects are difficult to accurately segment due to the limited image segmentation accuracy (see Fig. 9(c) ⑥). It also struggles to learn a discriminative embedding, especially for some objects with similar appearance but inconsistent identities (see Fig. 9(a) ②), which may lead to ambiguous tracking. Furthermore,

W. Ye, X. Lan, H. Bao, Z. Cui and G. Zhang are with the State Key Lab of CAD&CG, Zhejiang University, and affiliated with ZJU-SenseTime Joint Lab of 3D Vision. G. Su is with Zhejiang University. E-mails: {weicaiye, xinyuelan, suge, baohujun, zhpcui, zhangguofeng}@zju.edu.cn

\*: indicates equal contribution. G. Zhang is the corresponding author.

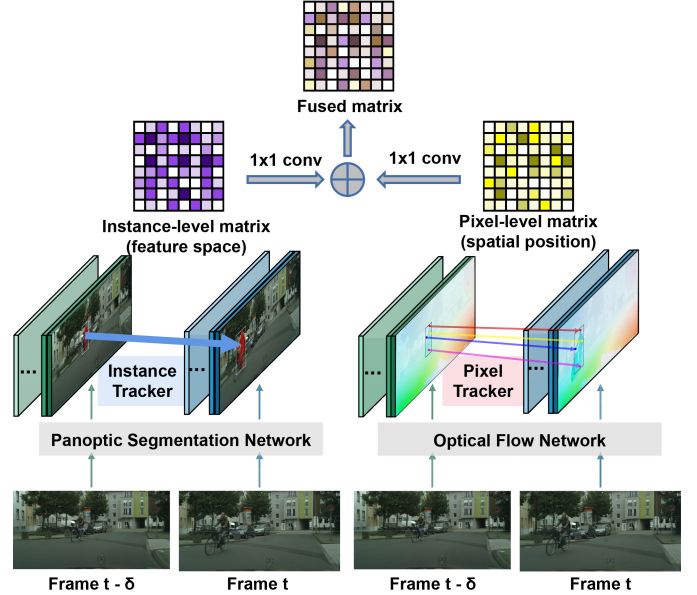


Fig. 1: **Brief illustration of HybridTracker.** HybridTracker achieves video panoptic segmentation from two perspectives: feature space (Instance Tracker) and spatial location (Pixel Tracker).

VPSNet uses optical flow estimation to fuse the features of adjacent frames to further improve the segmentation, which is undoubtedly heavy and complicated. Woo et al. [4] improved VPSNet by introducing the contrast loss and pixel-level tube-matching loss to obtain time-invariant features, while it still relies on the instance-level features for the tracking as VPSNet.

CenterTrack [5] proposed a simultaneous detection and tracking algorithm to localize objects and predict their associations by objects' centers, which can be considered a tracker based on pixels. However, the tracking is not stable enough due to the sparsity of the objects' center, especially in the face of multiple objects occlusion and reappearance after the disappearance. Moreover, it has not been applied to the video panoptic segmentation task. Existing instance-based and pixel-based trackers are particularly weak in handling multi-object occlusion (see Fig. 9(a) ③ and 9(c) ⑤) and large instance contour deformations (see Fig. 8 ③).

To address the problems aforementioned, we propose to track with both pixel and instance for video panoptic segmentation. Our insight is that VPS can benefit from different perspectives including feature space (instance tracker) and spatial location (pixel tracker), which can effectively mitigate the drawbacks of using a single-level tracker (see Fig. 1).

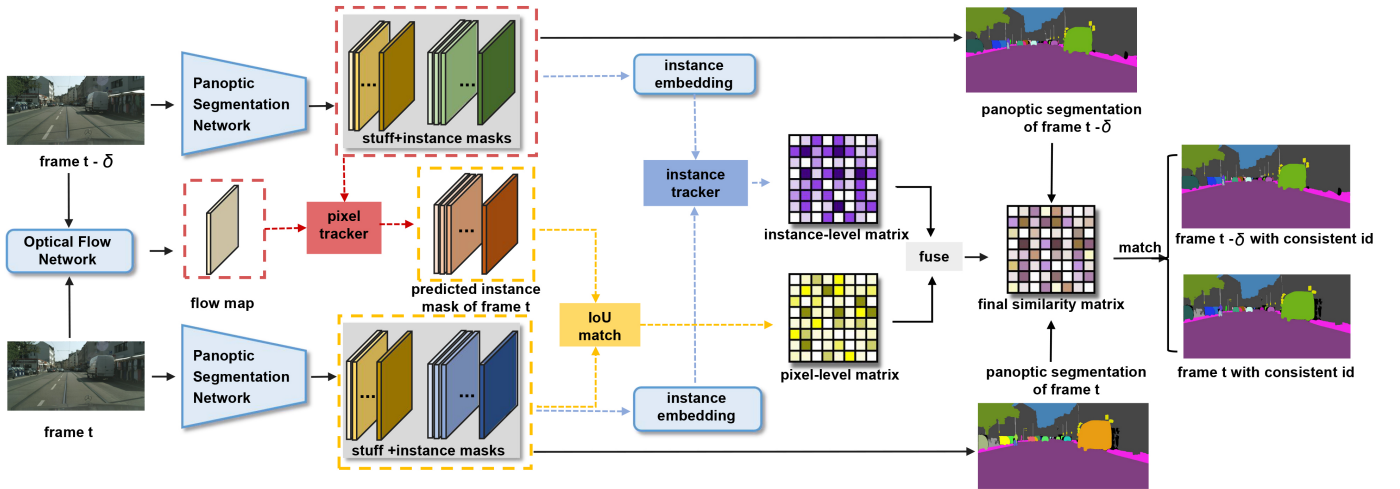


Fig. 2: **HybridTracker framework.** Our network takes consecutive video frames as input and outputs the segmentation results of each frame and the consistent tracking IDs between frames. Each frame is fed into the image panoptic segmentation network. Then instance tracker and pixel tracker are run to obtain the correlation matrices of instances between frames, which are finally fused into a matching matrix to obtain consistent video panoptic segmentation results.

However, directly combining the existing instance-based and pixel-based tracker is non-trivial. On the one hand, it leads to onerous network parameters, making the models much larger and harder to train on a standard graphics card. On the other hand, different trackers need to maintain a good tracking performance to obtain complimentary tracking effects through fusion. Otherwise, intermediate results will be obtained.

To achieve a trade-off between memory consumption and VPS performance, we propose a lightweight and joint tracking network, termed HybridTracker, (see Fig. 2). HybridTracker performs panoptic segmentation for each frame and adopts different trackers to obtain the correlation matrices fused into a final matching matrix to obtain the spatiotemporal consistent video panoptic segmentation results. Specifically, we use a lightweight image panoptic segmentation model PanopticFCN [6] to obtain the panoptic segmentation results for each frame, which can obtain competitive segmentation results with fewer parameters and faster speed. In the instance tracker, to reduce memory consumption, we take the segmented instance mask to obtain the ROI mask of each instance by cropping, scaling, and padding, and then leverage two fully connected layers to obtain the embedding of each instance.

To address the issue of training convergence that usually exists for the instance-based tracker [7], [8], we present a differentiable matching layer to obtain the correspondence between different instances and then train the network with the cross-entropy loss. In pixel tracker, rather than sparse objects' center in CenterTrack [5], we use the dense optical flow estimation network RAFT [9] to obtain the dense pixel motion of the current frame and add the original coordinate of pixels to obtain the mask of each instance in the next frame. The IoU matching matrix is obtained by computing the dice coefficient of the same instance of different frames.

To deal well with the irregular deformations caused by perspective projection and individual instances reappearing

after disappearing, we also propose mutual check and temporal consistency constraints applied to the proposed HybridTracker, which can effectively eliminate these issues. Our contributions can be briefly summarised as four-fold.

- We present a lightweight and efficient hybrid tracker network consisting of an instance tracker and a pixel tracker that effectively copes with video panoptic segmentation.
- Our differentiable matching module for instance tracker can smoothly train the embedding of instances and maintain tracking robustness. While our dense pixel tracker does not require additional training.
- Our proposed mutual track and temporal consistency constraints can effectively handle complex challenges such as reappearance after a disappearance due to occlusion and strong instance deformations.
- Extensive experiments demonstrate that HybridTracker achieves superior performance than state-of-the-art methods on Cityscapes-VPS and VIPER datasets.

## II. RELATED WORK

**Video Segmentation.** A comprehensive overview [10] of multiple tasks in video segmentation has recently been proposed, which broadly classifies video segmentation into eight tasks such as video semantic segmentation [11]–[14], interactive video object segmentation [15]–[17], semi-automatic video object segmentation [18]–[21], object-level automatic video object segmentation [22]–[25], language-guided video object segmentation [26]–[28], instance-level automatic video object segmentation [29], [30], video instance segmentation [3], [31]–[36], and video panoptic segmentation [1], [4], [37], [38]. Among them, it systematically describes the methods used in these tasks in recent years, the datasets used and the results achieved so far, as well as the future trends. In this work, we focus on video panoptic segmentation.

**Video Panoptic Segmentation.** The pioneering work of video panoptic segmentation – VPS [1] extends the panoptic

segmentation task from the image domain to the video domain, proposing an instance-level tracking-based approach. Based on this, SiamTrack [4] proposes pixel-tube matching loss and contrast loss, which improves the discriminative power of instance embedding further. These methods can be roughly considered as instance trackers. The contemporaneous work, STEP [38] proposes to directly segment and track each pixel of the video. In comparison, we propose a hybrid tracker, which consists of a pixel tracker and an instance tracker for video panoptic segmentation. Note that we focus on better tracking of the video segmentation results, rather than fusing the features of different frames to obtain better image segmentation results as in VPSNet [1]. We also add the mutual check and temporal consistency constraints to tackle the challenges of deformations and reappearance after occlusion. VIP-DeepLab [37] additionally introduces depth information to improve the performance of VPS, while our work focuses only on the video track without considering depth.

**Video Tracking.** Video segmentation requires consistent segmentation between consecutive frames, which is essentially the tracking of video elements. VPS [1] achieved this by tracking each instance from the perspective of feature space, while CenterTrack [5] through the center of each instance from the perspective of spatial location. No doubt that they struggle to handle some complex challenges, such as occlusion. A considerable amount of work [39]–[41] exists that focuses on multiple object tracking rather than video panoptic segmentation. QDTrack [40] proposed quasi-dense samples to track multiple objects, but it’s still based on feature space. Our proposed HybridTracker, which consists of an instance tracker and a dense pixel tracker, can robustly cope with the complex scenes for video panoptic segmentation from two perspectives: feature space and spatial location.

### III. METHODOLOGY

Given a monocular video, our target is to generate coherent video panoptic segmentation. To this end, we propose a lightweight and efficient network, termed HybridTracker (see Fig. 2) to tackle this problem. HybridTracker consists of four main components: an image panoptic segmentation network with shared weights, an instance tracker module with a differentiable matching layer, a dense pixel tracker module, and a final fusion module to obtain the matching matrix. To handle some complex challenges, we additionally add a mutual check and temporal consistency constraints to the instance tracker and pixel tracker during inference.

#### A. Image Panoptic Segmentation Network

Unlike VPSNet [1], which uses UPSNet [2] network based on Mask-RCNN [42], we choose PanopticFCN [6] to obtain the image panoptic segmentation for every video frame. PanopticFCN [6] is a simple and efficient network for panoptic segmentation, which represents background stuff and foreground things in a unified fully convolutional pipeline. As shown in Fig. 3, PanopticFCN leverages the kernel generator to embed each stuff category and object instance into a

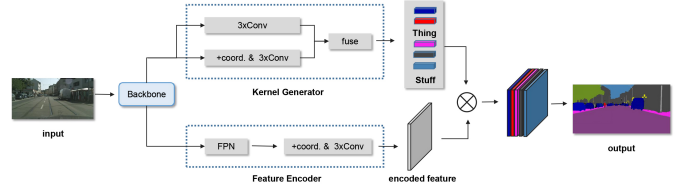


Fig. 3: **Image Panoptic Segmentation Network.** We take PanopticFCN [6] as the image panoptic segmentation network to produce the segmentation predictions with a unified representation of object instances or stuff categories given an RGB image.

specific kernel weight and generates the segmentation predictions. Compared with Mask-RCNN [42] used in VPS [1], PanopticFCN is a box-free method which is a memory and parameter-friendly network, and this makes our HybridTracker as lightweight as possible. We use the dice segmentation loss [43] and position loss as the basic loss.

The dice segmentation loss is defined as follows:

$$\mathcal{L}_{\text{seg}} = \sum_j \text{Dice}(\mathbf{P}_j, \mathbf{Y}_j^{\text{seg}}) / (M + N), \quad (1)$$

where  $\mathbf{Y}_j^{\text{seg}}$  is the  $j$ -th ground truth label of the prediction  $\mathbf{P}_j$ , while  $\mathbf{P}_j = K_j \otimes \mathbf{F}^e$ . The  $K_j$  is the kernel weights of  $M$  things  $K^{\text{th}}$  and  $N$  stuff  $K^{\text{st}}$ , while  $\mathbf{F}^e \in \mathbb{R}^{C_e \times W/4 \times H/4}$  is the encoded feature.

The position loss  $\mathcal{L}_{\text{pos}}$  is used to optimized the object centers with  $\mathcal{L}_{\text{pos}}^{\text{th}}$  and stuff regions with  $\mathcal{L}_{\text{pos}}^{\text{st}}$ :

$$\begin{aligned} \mathcal{L}_{\text{pos}}^{\text{th}} &= \sum_i \text{FL}(\mathbf{L}_i^{\text{th}}, \mathbf{Y}_i^{\text{th}}) / N_{\text{th}}, \\ \mathcal{L}_{\text{pos}}^{\text{st}} &= \sum_i \text{FL}(\mathbf{L}_i^{\text{st}}, \mathbf{Y}_i^{\text{st}}) / W_i H_i, \\ \mathcal{L}_{\text{pos}} &= \mathcal{L}_{\text{pos}}^{\text{th}} + \mathcal{L}_{\text{pos}}^{\text{st}}, \end{aligned} \quad (2)$$

where  $\text{FL}(\cdot, \cdot)$  denotes the Focal Loss [44].  $\mathbf{L}_i^{\text{th}} \in \mathbb{R}^{N_{\text{th}} \times W_i \times H_i}$  is the object map,  $\mathbf{L}_i^{\text{st}} \in \mathbb{R}^{N_{\text{st}} \times W_i \times H_i}$  is stuff map and  $\mathbf{Y}_i^{\text{st}} \in [0, 1]^{N_{\text{st}} \times W_i \times H_i}$  is the ground truth. The final basic loss is:

$$\mathcal{L}_{\text{base}} = \lambda_{\text{pos}} \mathcal{L}_{\text{pos}} + \lambda_{\text{seg}} \mathcal{L}_{\text{seg}}, \quad (3)$$

where  $\lambda_{\text{pos}}$  is 1.0 and  $\lambda_{\text{seg}}$  is 4.0.

#### B. Instance Tracker Module

After the images are fed into the image panoptic segmentation network, we can obtain each foreground object instance and background stuff, which can be used to learn the embedding of each instance for tracking between video frames. Unlike MaskTrack [3] which obtains a 28x28 mask based on the anchor, it is possible to directly use several fully connected layers to obtain the embedding of the corresponding instances. While PanopticFCN [6] obtains the mask of the original image, using the previous method directly may consume too much GPU memory and struggle to obtain good embedding. For an arbitrary two images frame  $t - \delta$  and frame  $t$ , assume that frame  $t - \delta$  has  $m$  instances, we transform the binary mask of each

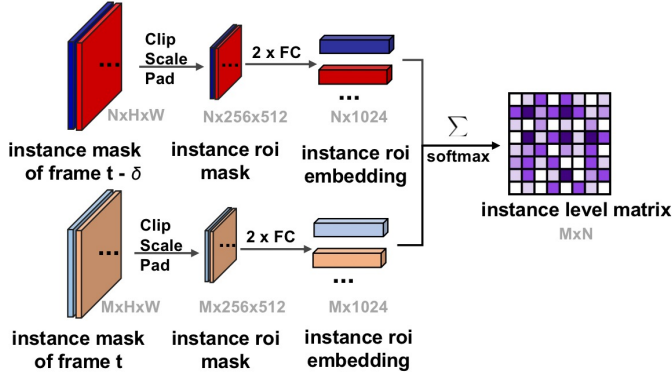


Fig. 4: **Instance Tracker Module.** Instance tracker takes each instance segmentation mask as input, crops, scales, and pads the predicted masks to the uniform size of masks, and two fully connected layers follow. We use the operation of  $M_{mn} = \sum a_{mk}b_{mk}$  and  $\text{softmax}$  to compute the instance similarity matrix.

instance into a bounding box, and crop the region enclosed by the bounding box into RoI feats, and then the RoI feature map is scaled to the shape of  $256 * 512$ , the empty regions are padded by 0, which ensures no deformation occurred when the RoI mask obtained. We get  $m * 1024$  embedding by two fully connected layers and yield an embedding of  $n * 1024$  for frame  $t$ , which has  $n$  instances. To calculate the similarity of each two instances of the two images, we multiply the embedding of each instance two by two to obtain  $m * n$  values, which forms the instance matching matrix  $M_{mn} = \sum a_{mk}b_{mk}$ . The instance tracker is detailed in Fig. 4. We can get the matching indexes simply through the operation of  $\text{torch.argmax}$ . We also used bipartite graph matching [45] to solve the instance correspondence and found less improvement, probably because the learned embedding is robust enough that it may not cause ambiguous matches.

**Instance-Wise Differentiable Matching layer based on Instance Embedding.** In the instance tracker, the instance embedding is trained to track the elements between frames. Existing methods use triplet loss [8] or contrast loss [4] to pull the same instance as close as possible in feature space and push different instances as far as possible. These methods identify nearest neighbor matches in feature space to establish instance correspondences, which are non-differentiable and unstable during training.

To address this issue, inspired by CAPS [46], we propose to use an instance-wise differentiable matching layer (DML) for the training of instance embedding. Given a set of frame  $t - \delta$  and frame  $t$ , the panoptic segmentation network with shared weights mentioned above obtains the embedding vectors  $M$  and  $N$  respectively. To compute the correspondence of the instance  $i$  in frame  $t - \delta$  to the frame  $t$ , we correlate the instance embedding, denoted  $M_i$ . Then, we use a 2D softmax operation to obtain the distribution of the different instances of frame  $t$ , which represents the probability that the instance

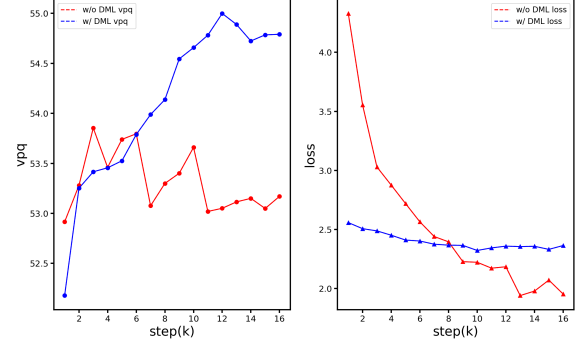


Fig. 5: **Training and testing of instance tracker w/ VS w/o the differentiable matching layer (DML).** DML helps instance tracker converge faster and more stable with higher VPQs.

of image frame  $t$  corresponds to the instance  $i$ :

$$p(\mathbf{j}|\mathbf{i}, \mathbf{M}, \mathbf{N}) = \frac{\exp(\mathbf{M}(\mathbf{i})^T \mathbf{N}(\mathbf{j}))}{\sum_{\mathbf{x} \in \mathbf{t}} \exp(\mathbf{M}(\mathbf{i})^T \mathbf{N}(\mathbf{x}))}, \quad (4)$$

where  $\mathbf{x}$  is the instance indexes of frame  $t$ . Then the predicted target  $\hat{\mathbf{j}}$  can be computed as the expectation of the distribution:

$$\hat{\mathbf{j}} = h_{t-\delta \rightarrow t}(\mathbf{i}) = \sum_{\mathbf{j} \in \mathbf{t}} \mathbf{j} \cdot p(\mathbf{j}|\mathbf{i}, \mathbf{M}, \mathbf{N}). \quad (5)$$

We use the cross-entropy loss to optimize the ground-truth target  $\mathbf{j}$  and the predicted target  $\hat{\mathbf{j}}$ , which is stable and easy to converge during the training process. The matching loss can be defined as follows:

$$\mathcal{L}_{\text{match}} = \frac{1}{M} \sum_{m=1}^M -(y \log(p) + (1 - y) \log(1 - p)), \quad (6)$$

where  $p$  represents the probability of correspondence between the ground-truth target  $\mathbf{j}$  and the predicted target  $\hat{\mathbf{j}}$ , i.e.,  $p(\mathbf{j}|\mathbf{i}, \mathbf{M}, \mathbf{N})$ .  $y$  is binary indicator if predicted target  $\hat{\mathbf{j}}$  is the correct classification for ground-truth target  $\mathbf{j}$ .

### C. Pixel Tracker Module

Pixel tracker can be considered as a tracker that maintains consistency in terms of the spatial position of the instances. Unlike CenterTrack [5] which exploits sparse objects' center to track multi-objects, we propose to track each instance by dense pixel motion. In pixel tracker (see Fig. 6), the images of two adjacent frames are fed into the optical flow estimation network, such as RAFT [9], to obtain the inter-frame motion information. Take the instance  $i$  in frame  $t - \delta$  as an example, we multiply the binary mask of instance  $i$  and flow map to get the motion of each pixel of instance  $i$ . Then, we add the coordinates of each pixel of the instance and the motion shift pixel by pixel to get the mask of each instance in the next frame. We can calculate the dice coefficient [43] values between the  $m$  instances in the frame  $t - \delta$  and the  $n$  instances

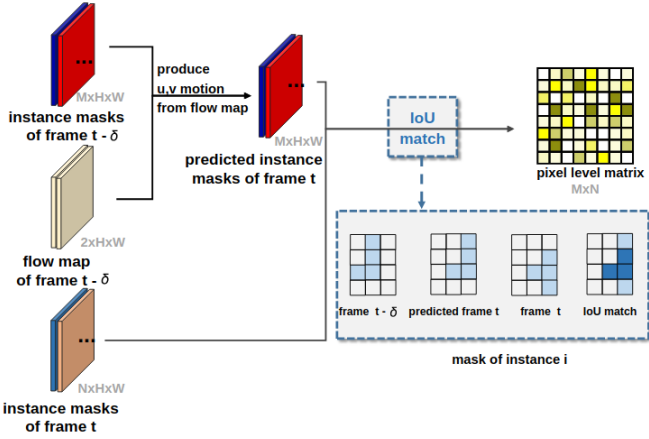


Fig. 6: **Pixel Tracker Module.** We calculate the dice coefficient of different instances from the frame  $t - \delta$  and frame  $t$  given the optical flow map, to form the position-aware similarity matrix.

in the frame  $t$  as the position similarity. The position similarity can be defined as follows:

$$Sim_{pos} = \frac{2 \sum_i^N p_i g_i}{\sum_i^N p_i^2 + \sum_i^N g_i^2}, \quad (7)$$

where  $p_i \in P$  means the predicted binary segmentation mask of instance  $i$  and  $g_i \in G$  means the predicted binary mask of instance  $i$ . Then we can form an  $m * n$  IoU correlation matrix, where  $m$  means the number of segmentation masks of the frame  $t - \delta$ , and  $n$  means the number of masks of the frame  $t$ .

#### D. Fusion Module

We take the two correlation matrices obtained by pixel tracker and instance tracker as input, feed them to a simple 1x1 Conv layer, and fuse them into a joint correlation matrix by adding them pixel by pixel to obtain the matching relationship between the two frames. The matching of instance IDs is obtained by taking the id of the largest column row by row, where matches probabilities less than a certain threshold, such as  $1e-5$ , are also removed, and a 1-to-1 matching constraint is added. For example, row  $i$  matches column  $j \rightarrow (i, j)$ , and the corresponding column  $j$  also should match row  $i \rightarrow (j, i)$ , which is considered a correct match. Matches that do not satisfy this constraint will be removed. Due to the large gap between the instance tracker and the pixel tracker, a simple fusion will only give intermediate results, while using our fusion module will generate better results, which also shows the effectiveness of our HybridTracker.

#### E. Mutual Check and Temporal Consistency Constraints

Although our HybridTracker can effectively solve the unstable tracking phenomenon of the single tracker, shown in Fig. 8(c), we found that we still cannot handle the complex deformation of some objects well. For this reason, we propose the mutual check which aims to remove inconsistent matches between two instances, and the temporal consistency

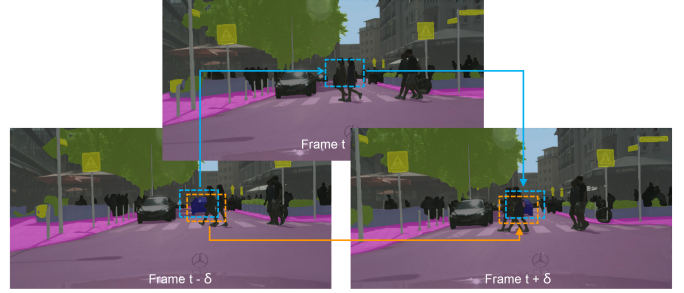


Fig. 7: **Illustration of temporal consistency constraint.** The car in the blue line box is incorrectly segmented in frame  $t$  due to occlusion, resulting in missing segmentation results. The blue line indicates that directly using the adjacent frame information may cause the tracking between frame  $t - \delta$  and frame  $t + \delta$  to fail. In comparison, the orange color line can address this limitation by the temporal consistency constraint.

constraints [47] which constrain the consistency of tracking between multiple frames in inference. Assume that  $\mathcal{T}$  is a differentiable operation  $x_t^p \mapsto x_s^p$ , which measures the similarity of  $x_s^p$  and  $x_t^p$ , where  $s$  and  $t$  indicate timestamp,  $p$  can be regarded as the spatial location of pixels or the feature of the instances. We can apply  $\mathcal{T}$  from  $t - \delta$  to  $t$  and from  $t$  to  $t + \delta$ , and the temporal consistency can be established:

$$\mathcal{T}(x_{t-\delta}^p, x_{t+\delta}^p) = \mathcal{T}(x_{t-\delta}^p, x_t^p) \mathcal{T}(x_t^p, x_{t+\delta}^p). \quad (8)$$

An obvious example illustrates that the temporal consistency constraint can robustly settle the issues of multi-object occlusion and missing segmentation of individual instances in the video sequence, shown in Fig. 7. In inference, since the car in frame  $t + \delta$  fails to find a matching instance in frame  $t$ , we obtain the frame  $t - \delta$  stored in memory and use our tracker (instance tracker or pixel tracker or hybrid tracker) to obtain the similarity matrix between frame  $t - \delta$  and  $t + \delta$ . If the similarity value is greater than the specific threshold, we will adopt temporal matches. Otherwise, the new instance id will be set. By the way, the temporal consistency constraint should be further applied backward from time  $t + \delta$  to  $t$  and from  $t$  to  $t - \delta$ . This temporal consistency constraint can also be used for other sequence problems to ensure consistency.

## IV. IMPLEMENTATION DETAILS

We first pre-train the image panoptic segmentation network, PanopticFCN [6] without tracking functionality on the Cityscapes-VPS and VIPER datasets and implement our models with the Pytorch-based toolbox Detectron2<sup>1</sup>. Following VPSNet-Track [1], we adopt the same multi-scale inference scaling equal to 0.5, 0.625, 0.6875, 0.8125, 0.875, 1. The resolution of the Cityscapes image is  $1024 \times 2048$ , while the VIPER image is  $1080 \times 1920$ . We optimize the network with an initial rate of 0.0025 on 4 GeForce GTX TITAN X GPUs, where each mini-batch has four images. We use the SGD optimizer with weight decay  $1e-4$  and momentum 0.9. Then we finetune the instance tracker with the differentiable

<sup>1</sup><https://github.com/facebookresearch/detectron2>

TABLE I: **Quantitative comparisons of video panoptic segmentation on Cityscapes-VPS validation (top) and test (bottom) Set. Our methods generally outperforms VPSNet-FuseTrack [1] and SiamTrack [4].** Each cell contains VPQ / VPQ<sup>Th</sup> / VPQ<sup>St</sup> scores. The best results are highlighted in boldface. **Note** that the configuration of our method is consistent with VPSNet-Track.

Methods on <b>Cityscapes-VPS val</b>	Temporal window size				VPQ	FPS
	k = 0	k = 5	k = 10	k = 15		
VPSNet-Track	63.1 / 56.4 / 68.0	56.1 / 44.1 / 64.9	53.1 / 39.0 / 63.4	51.3 / 35.4 / 62.9	55.9 / 43.7 / 64.8	4.5
VPSNet-FuseTrack	64.5 / 58.1 / 69.1	57.4 / 45.2 / 66.4	54.1 / 39.5 / 64.7	52.2 / 36.0 / 64.0	57.2 / 44.7 / 66.6	1.3
SiamTrack	64.6 / 58.3 / 69.1	57.6 / 45.6 / 66.6	54.2 / 39.2 / 65.2	52.7 / 36.7 / 64.6	57.3 / 44.7 / 66.4	4.5
Instance Tracker	65.6 / 60.0 / 69.7	55.1 / 39.3 / 66.6	51.4 / 32.5 / 65.1	49.3 / 28.6 / 64.3	55.3 / 40.1 / 66.4	5.1
Pixel Tracker	65.6 / 60.0 / 69.7	58.8 / 48.0 / 66.6	55.4 / 42.1 / 65.1	53.2 / 38.0 / 64.3	58.2 / 47.0 / 66.4	3.8
HybridTracker (Instance + Pixel)	65.6 / 60.0 / 69.7	58.9 / 48.3 / 66.6	55.6 / 42.5 / 65.1	53.4 / 38.5 / 64.3	58.4 / 47.3 / 66.4	3.6
HybridTracker + w/ Temporal	<b>65.6</b> / 60.0 / 69.7	<b>59.0</b> / 48.5 / 66.6	<b>55.7</b> / 42.8 / 65.1	<b>53.6</b> / 38.9 / 64.3	<b>58.5</b> / 47.5 / 66.4	3.3

Methods on <b>Cityscapes-VPS test</b>	Temporal window size				VPQ	FPS
	k = 0	k = 5	k = 10	k = 15		
VPSNet-Track	63.1 / 58.0 / 66.4	56.8 / 45.7 / 63.9	53.6 / 40.3 / 62.0	51.5 / 35.9 / 61.5	56.3 / 45.0 / 63.4	4.5
VPSNet-FuseTrack	64.2 / 59.0 / 67.7	57.9 / 46.5 / 65.1	54.8 / 41.1 / 63.4	52.6 / 36.5 / 62.9	57.4 / 45.8 / 64.8	1.3
SiamTrack	63.8 / 59.4 / 66.6	58.2 / 47.2 / 65.9	56.0 / 43.2 / 64.4	<b>54.7</b> / 40.2 / 63.2	57.8 / 47.5 / 65.0	4.5
Instance Tracker	61.7 / 56.2 / 65.2	55.0 / 43.0 / 62.6	52.2 / 38.1 / 61.2	50.3 / 34.4 / 60.5	54.8 / 42.9 / 62.4	5.1
Pixel Tracker	64.2 / 58.9 / 67.7	58.4 / 48.0 / 65.1	55.6 / 43.3 / 63.4	53.8 / 39.7 / 62.9	58.0 / 47.5 / 64.8	3.8
HybridTracker (Instance + Pixel)	64.3 / 58.9 / 67.7	58.6 / 48.5 / 65.1	55.8 / 43.9 / 63.4	54.1 / 40.2 / 62.9	58.2 / 47.9 / 64.8	3.6
HybridTracker + w/ Temporal	<b>64.3</b> / 59.0 / 67.7	<b>59.0</b> / 49.2 / 65.1	<b>56.3</b> / 45.0 / 63.4	54.5 / 41.4 / 62.9	<b>58.5</b> / 48.7 / 64.8	3.3

TABLE II: **Quantitative comparisons of video panoptic segmentation on VIPER. Our methods generally outperforms VPSNet-FuseTrack [1] and SiamTrack [4].** Each cell contains VPQ / VPQ<sup>Th</sup> / VPQ<sup>St</sup> scores. The best results are highlighted in boldface. **Note** that the configuration of our method is consistent with VPSNet-Track.

Methods on <b>VIPER</b>	Temporal window size				VPQ	FPS
	k = 0	k = 5	k = 10	k = 15		
VPSNet-Track	48.1 / 38.0 / 57.1	49.3 / 45.6 / 53.7	45.9 / 37.9 / 52.7	43.2 / 33.6 / 51.6	46.6 / 38.8 / 53.8	5.1
VPSNet-FuseTrack	49.8 / 40.3 / 57.7	51.6 / 49.0 / 53.8	47.2 / 40.4 / 52.8	45.1 / 36.5 / 52.3	48.4 / 41.6 / 53.2	1.6
SiamTrack	51.1 / 42.3 / 58.5	<b>53.4</b> / 51.9 / 54.6	49.2 / 44.1 / 53.5	47.2 / 40.3 / 52.9	50.2 / 44.7 / 55.0	5.1
Instance Tracker	55.1 / 51.2 / 58.0	45.7 / 30.4 / 57.5	43.8 / 26.2 / 57.3	41.5 / 21.5 / 57.0	46.5 / 32.3 / 57.5	5.7
Pixel Tracker	<b>55.1</b> / 51.2 / 58.0	52.2 / 45.4 / 57.5	50.9 / 42.4 / 57.3	49.5 / 39.9 / 57.0	51.9 / 44.7 / 57.5	3.8
HybridTracker (Instance + Pixel)	55.0 / 51.2 / 58.0	52.4 / 45.7 / 57.5	51.0 / 42.8 / 57.3	49.8 / 40.4 / 57.0	52.1 / 45.1 / 57.5	3.6
HybridTracker + w/ Temporal	55.0 / 51.2 / 58.0	52.6 / 46.2 / 57.5	<b>51.5</b> / 43.9 / 57.3	<b>50.4</b> / 42.0 / 57.0	<b>52.4</b> / 45.8 / 57.5	3.5

matching layer on the Cityscapes and VIPER datasets. For finetuning our instance tracker, we optimize the network with initial rate 1e-4 and 2 GeForce GTX TITAN X GPUs, where each mini-batch has 16 images. The pixel-tracker does not need training, which loads the pre-trained model weight from the optical flow network. We compose the instance tracker and the pixel tracker to the hybrid tracker to fuse the matching matrix. We also add a mutual check and temporal consistency constraints during inference.

## V. EXPERIMENT

### A. Datasets

We extensively perform experiments on two VPS datasets, including Cityscapes-VPS datasets and VIPER datasets. For fair comparison, we follow VPS [1] and use its public train/val/test split of these datasets. Each video of the Cityscapes-VPS consists of thirty consecutive frames with every five frames having ground truth annotation, a total of 6 frames are annotated. VIPER is another high-quantity and quality video panoptic segmentation benchmark. Following VPS [1], We select the first 60 frames of 10 videos of the day scenarios as the validation set, with a total of 600 images.

### B. Experimental Details

We consider Cityscapes-VPS as a primary evaluation dataset as the dataset is relatively small, which allows us to quickly

validate our various experimental settings, and then we analogize our learned knowledge to the VIPER dataset, which also shows consistent results.

We selected three instance-based video panoptic segmentation methods as comparison, including VPSNet-Track, VPSNet-FuseTrack [1] and SiamTrack [4]. VPSNet-Track is a video panoptic segmentation baseline that adds MaskTrack head [3] on top of the single image panoptic segmentation model, UPSNet [2]. VPSNet-FuseTrack based on VPSNet-Track, adds temporal feature aggregation and fusion module to improve the performance of video panoramic segmentation. SiamTrack [4] finetunes VPSNet-Track with the pixel-tube matching loss and the contrast loss and is only slightly better than VPSNet-FuseTrack. We mainly compare with VPSNet-FuseTrack<sup>2</sup> for SiamTrack's source code is not publicly available. The VPQ results are from SiamTrack [4].

To better evaluate the joint tracking network, we experiment with the proposed instance tracker, pixel tracker, and hybrid tracker respectively. We additionally add a mutual check and temporal consistency constraints to the single and hybrid tracker. The VPQ metric [1] is adopted to evaluate the spatial-temporal consistency between the ground truth and predicted video panoptic segmentation.

<sup>2</sup><https://github.com/mcahny/vps>

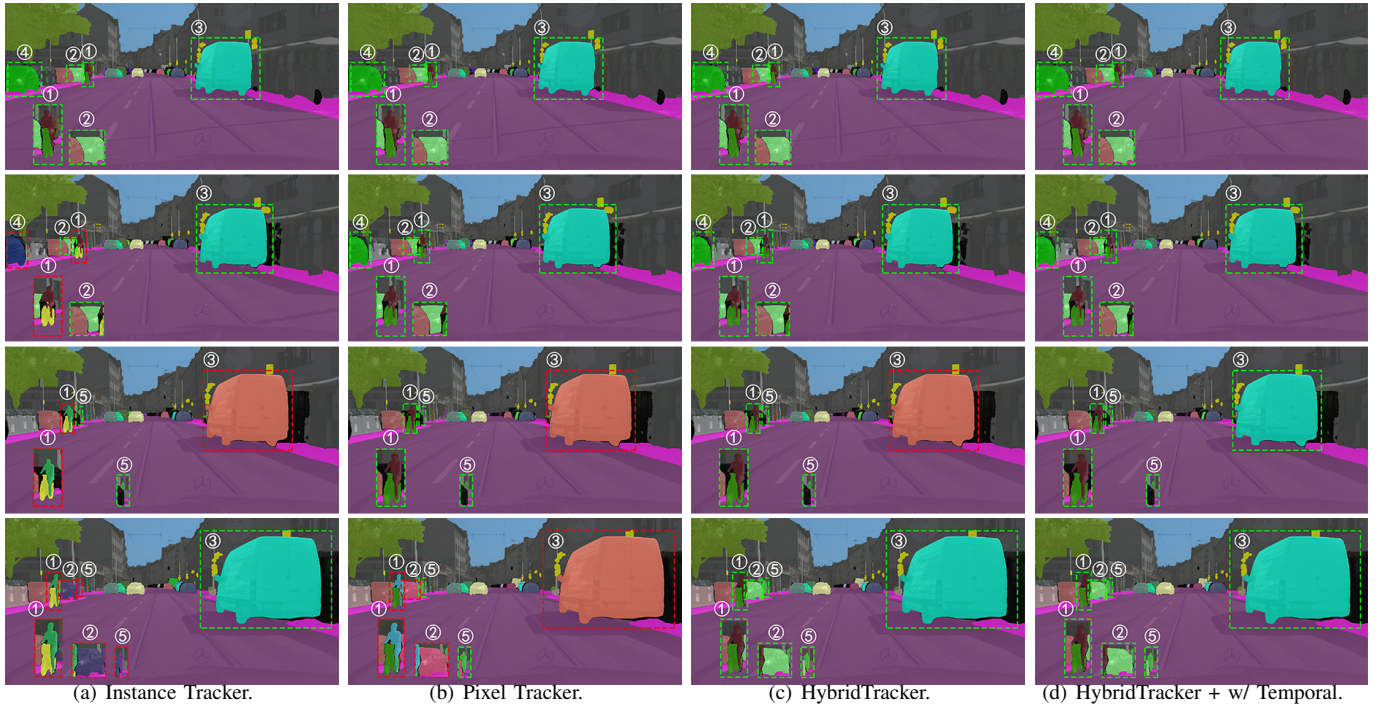


Fig. 8: **Illustration of our different trackers on Cityscapes-VPS dataset.** Each column with the same marker indicates a tracking instance. The green box indicates correct tracking, while the red box indicates false tracking. Instance Tracker can handle large objects with minor contour deformation but struggles to handle small objects. In contrast, Pixel Tracker can handle small objects with limited motion, rather than irregular motion (④ and ⑤). HybridTracker is expert in settling small objects with large motion (① and ②). The temporal consistency constraints help track small and large objects with occlusion and inter-frame jump due to deformation (③).

### C. Main Results

1) *Cityscapes-VPS*: Tab. I summarizes video panoptic segmentation (VPQ) results of all methods on the Cityscapes-VPS val and test dataset. We observed that our Instance Tracker is on par with Track, while Pixel Tracker is better than VPSNet-FuseTrack, which makes our full HybridTracker outperform VPSNet-FuseTrack, and achieve faster inference (**3.6FPS** vs. 1.3FPS) and fewer parameters (**170.8MB** vs. 214.9MB). Furthermore, HybridTracker with temporal consistency constraint has further improvements, outperforming VPSNet-FuseTrack with **+1.3% VPQ** gain for the val dataset and **+1.1% VPQ** gain for the test dataset. **Note** that all our model does not fuse feature from consecutive frames like VPSNet-FuseTrack [1]. In addition, we combine better panoptic segmentation results from VPSNet-FuseTrack with our pixel tracker on the Cityscapes-VPS val dataset to achieve better VPQ scores, compared with VPSNet-FuseTrack. Fig. 9 demonstrates that compared with VPSNet-FuseTrack, HybridTracker can robustly handle multiple object occlusions (① and ③) and similar appearance but different identities (②) and maintain robust tracking even for small objects such as a person on a motorcycle (④), a car (⑥), and a car obscured by a utility pole (⑤). The reason why HybridTracker does not have a big improvement over Pixel Tracker is that Pixel Tracker is relatively robust, and the proportion of bad cases is not too large. In addition, there is still a big gap between Instance Tracker and Pixel Tracker in performance, and simple

fusion can only get intermediate results, which also reflects the effectiveness of our HybridTracker.

2) *VIPER*: Tab. II summarizes the VPQ results of all the methods on VIPER datasets, and we observe a consistent tendency. Compared with VPSNet-FuseTrack, our HybridTracker model with pixel and instance tracker module achieves much higher scores (**52.1VPQ** vs. 48.4 VPQ) using the learned ROI feature matching algorithm and the spatial position correlation cues. Our HybridTracker with the mutual check and temporal consistency constraints achieves the best performance by improving **+4.0% VPQ** over VPSNet-FuseTrack, and runs at a much faster inference speed (2x).

### D. Ablation Study

1) *Analysis on HybridTracker*: We evaluate the VPQ performance of different variants of our methods. From Tab. I and Tab. II, the proposed instance tracker is slightly worse than VPSNet-FuseTrack [1]. To be fair to the existing method, VPSNet, our instance tracker is not specifically optimized and can run faster with fewer parameters to get comparable results. While the pixel tracker model greatly outperforms instance-tracker methods. The HybridTracker achieves the best results owing to the fusion module. Fig. 8 shows the qualitative results of our methods on Cityscapes-VPS. The qualitative results on the VIPER dataset shown in Fig. 10 demonstrate that HybridTracker is expert in settling small objects with large motion (① and ②). In addition, the temporal consistency



Fig. 9: **Comparison results of our methods with VPSNet-FuseTrack [1] on Cityscapes-VPS val and test dataset.** Each column with the same marker indicates a tracking instance. The green box indicates correct tracking, while the red box indicates false tracking. Compared with VPSNet-FuseTrack, HybridTrack can robustly handle multiple object occlusions (① and ③) and similar appearance but different identities (②) on the val dataset and maintain robust tracking on the test dataset even for small objects such as a person on a motorcycle (④), a car (⑥), and a car obscured by a utility pole (⑤).

constraints help track small and large objects with occlusion and inter-frame jump due to deformation (③).

2) **Analysis on Differentiable Matching Layer in Instance Tracker:** To verify the effect of this layer, we explore the performance of instance embedding with various loss functions. Experiments show that our method can be trained more smoothly and can converge faster than the existing contrast loss with higher VPQ scores, shown in Fig. 5.

3) **Analysis on RAFT Version and Iterations:** In Pixel Tracker, we calculate the dice coefficient of different instances from the frame  $t - \delta$  and frame  $t$  given the optical flow map to form the position-aware similarity matrix. We use the flow estimation network RAFT to estimate the optical flow from two consecutive frames. The source code of RAFT is released with five versions of pre-trained weights. We performed ablation studies on different versions of RAFT to understand the impact on the pixel tracker, shown in Table III. The sintel version of RAFT achieves the best performance, for MIP Sintel is a large synthetic dataset that provides detailed and dense optical flow annotation, and it contains many challenging scenes, making it a good generalization capability. We perform different iterations on the raft-sintel to understand the impact on the pixel tracker, shown in Tab. IV. RAFT with 20 iterations achieves the best performance.

4) **Analysis on Mutual Check and Temporal Consistency Constraints:** We also conducted additional experiments on the mutual check and temporal consistency constraints with ablation consideration. All of our methods (including Instance

TABLE III: **Ablation study of different versions of RAFT, which affects pixel tracker on Cityscapes-VPS validation dataset.** The best results are highlighted in boldface.

version	PQ	PQ <sup>Th</sup>	PQ <sup>St</sup>
raft-chairs	57.01	44.08	66.42
raft-kitti	56.97	43.98	66.42
raft-sintel	<b>57.39</b>	<b>44.97</b>	<b>66.42</b>
raft-smalll	57.09	44.26	66.42
raft-things	57.35	44.87	66.42

TABLE IV: **Ablation study of different iterations on sintel version of RAFT, which affects Pixel Tracker on Cityscapes-VPS val dataset.** The best results are highlighted in boldface.

Iterations	PQ	PQ <sup>Th</sup>	PQ <sup>St</sup>	FPS
1	57.74	45.81	66.42	4.06
5	58.18	46.85	66.42	3.33
10	58.26	47.03	66.42	2.21
15	58.27	47.06	66.42	1.52
20	<b>58.37</b>	<b>47.31</b>	<b>66.42</b>	1.21
25	58.29	47.11	66.42	0.95

Tracker, Pixel Tracker, and HybridTracker) with mutual check and temporal consistency constraints achieve different levels of improvement of VPQs, illustrated in Tab. V and VI. Fig. 10 and 12 demonstrate the improvements of the temporal consistency constraint. In addition, we combine better panoptic

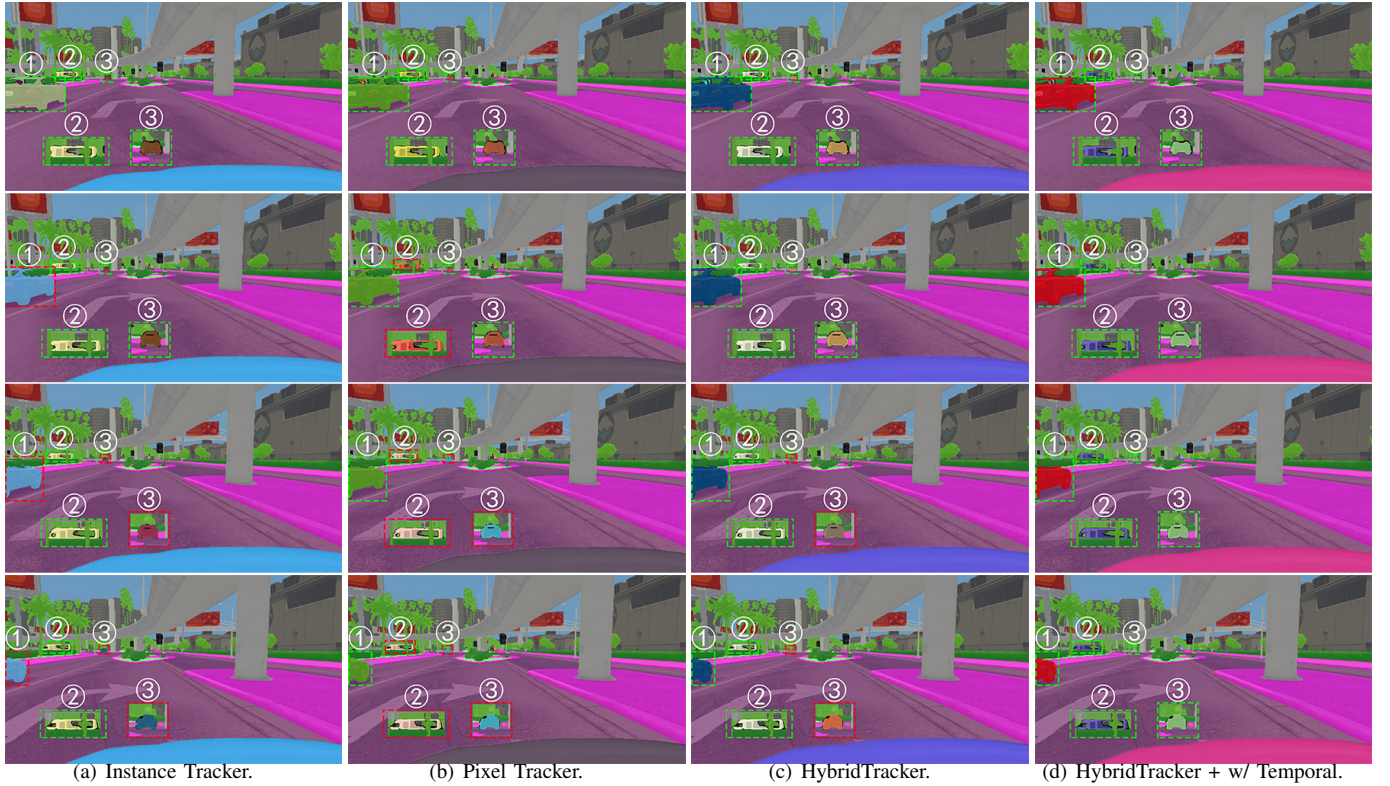


Fig. 10: **Illustration of our different trackers on VIPER dataset.** Instance Tracker can handle large objects (with minor contour deformation but struggles to handle small objects (②). In contrast, Pixel Tracker can handle small objects with limited motion, rather than irregular motion (①). HybridTracker is expert in settling small objects with large motion (① and ②). The temporal consistency constraints help track small and large objects with occlusion and inter-frame jump due to deformation (③).

TABLE V: **Ablaton study of temporal consistency constraints on Cityscapes-VPS validation set with our method variants.** Each cell contains VPQ / VPQ<sup>Th</sup> / VPQ<sup>St</sup> scores. The best results are highlighted in boldface. Note that the configuration of our method is consistent with VPSNet-Track. All trackers with temporal consistency constraints have improved performance. The combination of VPSNet-FuseTrack and our pixel tracker with temporal consistency constraint outperforms VPSNet-FuseTrack. Our HybridTracker with temporal consistency constraint achieves the best VPQ scores.

Methods on Cityscapes-VPS val.	Temporal window size				VPQ	FPS
	k = 0	k = 5	k = 10	k = 15		
VPSNet-Track	63.1 / 56.4 / 68.0	56.1 / 44.1 / 64.9	53.1 / 39.0 / 63.4	51.3 / 35.4 / 62.9	55.9 / 43.7 / 64.8	4.5
VPSNet-FuseTrack	64.5 / 58.1 / 69.1	57.4 / 45.2 / 66.4	54.1 / 39.5 / 64.7	52.2 / 36.0 / 64.0	57.2 / 44.7 / 66.6	1.3
SiamTrack	64.6 / 58.3 / 69.1	57.6 / 45.6 / 66.6	54.2 / 39.2 / 65.2	52.7 / 36.7 / 64.6	57.3 / 44.7 / 66.4	4.5
Instance Tracker	65.6 / 60.0 / 69.7	55.1 / 39.3 / 66.6	51.4 / 32.5 / 65.1	49.3 / 28.6 / 64.3	55.3 / 40.1 / 66.4	5.1
Instance Tracker + w/ Mutual Check	65.6 / 60.0 / 69.7	55.0 / 39.2 / 66.6	51.5 / 32.7 / 65.1	49.4 / 28.9 / 64.3	55.37 / 40.18 / 66.42	5.0
Instance Tracker + w/ Temporal	65.3 / 59.3 / 69.7	55.2 / 39.6 / 66.6	51.6 / 33.0 / 65.1	49.4 / 29.0 / 64.3	55.38 / 40.21 / 66.42	4.9
Instance Tracker + w/ Mutual + Temporal	65.3 / 59.4 / 69.7	55.2 / 39.5 / 66.6	51.7 / 33.2 / 65.1	49.6 / 29.3 / 64.3	55.44 / 40.35 / 66.42	4.8
Pixel Tracker	65.6 / 60.0 / 69.7	58.8 / 48.0 / 66.6	55.4 / 42.1 / 65.1	53.2 / 38.0 / 64.3	58.24 / 47.0 / 66.42	3.8
Pixel Track + w/ Temporal	65.6 / 60.0 / 69.7	58.9 / 48.3 / 66.6	55.5 / 42.4 / 65.1	53.3 / 38.2 / 64.3	58.34 / 47.1 / 66.42	3.6
HybridTracker (Instance + Pixel)	65.6 / 60.0 / 69.7	58.9 / 48.3 / 66.6	55.6 / 42.5 / 65.1	53.4 / 38.5 / 64.3	58.37 / 47.3 / 66.4	3.6
HybridTracker + w/ Temporal	<b>65.6</b> / 60.0 / 69.7	<b>59.0</b> / 48.5 / 66.6	<b>55.7</b> / 42.8 / 65.1	<b>53.6</b> / 38.9 / 64.3	<b>58.47</b> / 47.5 / 66.4	3.3
VPSNet-FuseTrack + Pixel	65.0 / 58.9 / 69.4	57.7 / 45.4 / 66.7	54.7 / 39.9 / 65.6	53.1 / 36.5 / 65.3	57.6515 / 45.1600 / 66.7363	1.1
VPSNet-FuseTrack + Pixel + w/ Temporal	65.0 / 58.9 / 69.4	57.7 / 45.4 / 66.7	54.8 / 39.9 / 65.6	53.1 / 36.5 / 65.3	57.6524 / 45.1619 / 66.7463	0.9

TABLE VI: Ablation study of temporal consistency constraints on VIPER dataset with our method variants. Each cell contains VPQ / VPQ<sup>Th</sup> / VPQ<sup>St</sup> scores. The best results are highlighted in boldface. Note that the configuration of our method is consistent with VPSNet-Track. All trackers with temporal consistency constraints have improved performance. Our HybridTracker with temporal consistency constraint achieves the best VPQ scores.

Methods on VIPER	Temporal window size				VPQ	FPS
	k = 0	k = 5	k = 10	k = 15		
VPSNet-Track	48.1 / 38.0 / 57.1	49.3 / 45.6 / 53.7	45.9 / 37.9 / 52.7	43.2 / 33.6 / 51.6	46.6 / 38.8 / 53.8	5.1
VPSNet-FuseTrack	49.8 / 40.3 / 57.7	51.6 / 49.0 / 53.8	47.2 / 40.4 / 52.8	45.1 / 36.5 / 52.3	48.4 / 41.6 / 53.2	1.6
SiamTrack	51.1 / 42.3 / 58.5	<b>53.4</b> / 51.9 / 54.6	49.2 / 44.1 / 53.5	47.2 / 40.3 / 52.9	50.2 / 44.7 / 55.0	5.1
Instance Tracker	55.1 / 51.2 / 58.0	45.7 / 30.4 / 57.5	43.8 / 26.2 / 57.3	41.5 / 21.5 / 57.0	46.53 / 32.33 / 57.45	5.7
Instance Tracker + w/ Temporal	54.4 / 49.7 / 58.0	46.1 / 31.3 / 57.5	44.4 / 27.6 / 57.3	42.3 / 23.2 / 57.0	46.79 / 32.95 / 57.45	5.5
Pixel Tracker	<b>55.1</b> / 51.2 / 58.0	52.2 / 45.4 / 57.5	50.9 / 42.4 / 57.3	49.5 / 39.9 / 57.0	51.92 / 44.73 / 57.45	3.8
Pixel Tracker + w/ Temporal	55.0 / 51.2 / 58.0	52.5 / 46.0 / 57.5	51.3 / 43.4 / 57.3	50.2 / 41.3 / 57.0	52.24 / 45.48 / 57.45	3.7
HybridTracker	55.0 / 51.2 / 58.0	52.4 / 45.7 / 57.5	51.0 / 42.8 / 57.3	49.8 / 40.4 / 57.0	52.06 / 45.05 / 57.45	3.6
HybridTracker + w/ Temporal	55.0 / 51.2 / 58.0	52.6 / 46.2 / 57.5	<b>51.5</b> / 43.9 / 57.3	<b>50.4</b> / 41.9 / 57.0	<b>52.39</b> / 45.80 / 57.45	3.5

TABLE VII: Ablation study of the different trackers under different temporal thresholds on Cityscapes-VPS validation dataset. Each cell contains VPQ / VPQ<sup>Th</sup> / VPQ<sup>St</sup> scores. The best results are highlighted in boldface. The change of the thresholds of temporal is not sensitive to VPQs.

Methods on Cityscapes-VPS val.	Temporal Thresholds $\theta$				
	$\theta = 0.001$	$\theta = 0.005$	$\theta = 0.01$	$\theta = 0.015$	$\theta = 0.02$
Instance Tracker	55.435/40.331/66.420	<b>55.445</b> /40.355/66.420	55.444/40.353/66.420	55.441/40.344/66.420	55.440/40.342/66.420
Pixel Tracker	57.467/45.157/66.420	57.467/45.157/66.420	<b>57.468</b> /45.160/66.420	57.468/45.160/66.420	57.468/45.160/66.420
HybridTracker	57.564/45.387/66.420	57.565/45.389/66.420	<b>57.568</b> /45.398/66.420	57.568/45.398/66.420	57.568/45.398/66.420



(a) Instance Tracker.



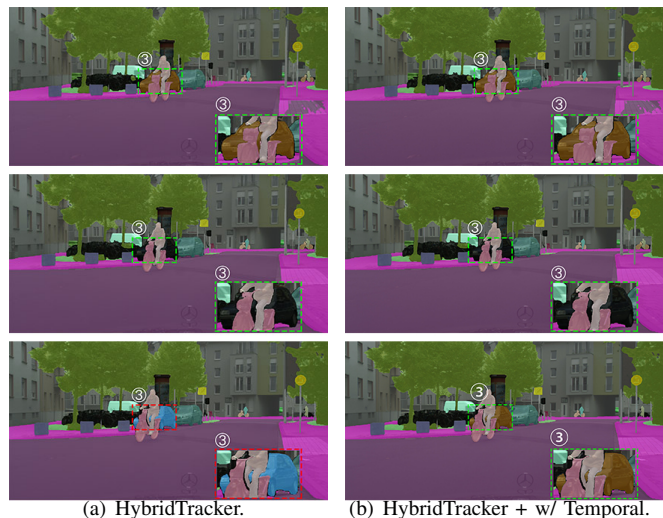
(b) Pixel Tracker.



(c) HybridTracker.

Fig. 11: Ablation study of different trackers on Cityscapes-VPS validation dataset. The same color of instance masks means the same instance. The green dashed boxes indicate the instances are correctly matched, while the red dashed boxes indicate false matches. Instance Tracker can handle large objects with more minor contour deformations (②) but struggles to handle small objects. In contrast, the pixel tracker can handle small objects with limited motions (①). HybridTracker can robustly settle these two cases (① and ②).

segmentation results from VPSNet-FuseTrack [1] with our Pixel Tracker on the Cityscapes-VPS validation dataset to achieve better VPQ scores. Our HybridTracker with tem-



(a) HybridTracker.

(b) HybridTracker + w/ Temporal.

Fig. 12: HybridTrack w/o vs w/ temporal consistency constraint on Cityscapes-VPS. The car in the second image cannot be segmented due to occlusion, resulting in a new id, while the temporal consistency constraint can circumvent this problem (③).

poral consistency constraint achieves the best performance on Cityscapes-VPS and VIPER validation datasets, shown in Tab. V and VI.

5) *Analysis on Temporal Thresholds*: We propose mutual check and temporal consistency constraints in inference to effectively address complex challenges, such as occlusion and strong contour deformations. We randomly select 3 images to form the image set, respectively: frame  $t - \delta$ , frame  $t$ , and frame  $t + \delta$ . To strengthen the matching relationship between adjacent size frames and reduce false matches across frames, the

temporal consistency constraint requires that: only when the similarity values of frame  $t-\delta$  and frame  $t+\delta$  are greater than a certain threshold, a cross-frame matching relationship will be established, assigning the ID of instance  $i$  in frame  $t-\delta$  to the ID of instance  $j$  in frame  $t+\delta$ . We set the thresholds to 0.001, 0.005, 0.01, 0.015 and 0.02. As shown in Tab. VII, the temporal consistency thresholds do not have a great impact on VPQ results.

## VI. CONCLUSION

We propose a lightweight and efficient hybrid tracker network consisting of an instance tracker and pixel tracker that effectively copes with video panoptic segmentation. Our proposed differentiable matching layer makes the instance tracker training stable and converges fast, while the dense pixel tracker can settle the small objects with smooth motion. The mutual check and temporal consistency constraints can effectively address complex challenges, such as occlusion and strong contour deformations. Comprehensive experiments show that HybridTracker achieves superior performance than state-of-the-art methods on Cityscapes-VPS and VIPER datasets.

**Limitations.** At first, the speed and accuracy of the tracking in our method are restricted to the optical flow estimation, while we find that RAFT [9] performs well on all datasets. The performance and efficiency of our method can be further improved with more advanced optical flow estimation methods. Second, our work focuses only on improving the tracking of individual instances rather than fusion for better segmentation results. Thus the mutual promotion of tracking and segmentation is a worthwhile direction to investigate.

## REFERENCES

- [1] D. Kim, S. Woo, J.-Y. Lee, and I. S. Kweon, "Video Panoptic Segmentation," in *Proceedings of the IEEE Conference on Computer Vision and Pattern Recognition (CVPR)*, 2020.
- [2] Y. Xiong, R. Liao, H. Zhao, R. Hu, M. Bai, E. Yumer, and R. Urtasun, "UPSNet: A Unified Panoptic Segmentation Network," in *Proceedings of the IEEE/CVF Conference on Computer Vision and Pattern Recognition (CVPR)*, 2019, pp. 8818–8826.
- [3] L. Yang, Y. Fan, and N. Xu, "Video Instance Segmentation," in *Proceedings of the IEEE/CVF International Conference on Computer Vision (ICCV)*, 2019, pp. 5188–5197.
- [4] S. Woo, D. Kim, J.-Y. Lee, and I. S. Kweon, "Learning to Associate Every Segment for Video Panoptic Segmentation," in *Proceedings of the IEEE/CVF Conference on Computer Vision and Pattern Recognition (CVPR)*, 2021, pp. 2705–2714.
- [5] X. Zhou, V. Koltun, and P. Krähenbühl, "Tracking Objects as Points," in *Proceedings of the European Conference on Computer Vision (ECCV)*. Springer, 2020, pp. 474–490.
- [6] Y. Li, H. Zhao, X. Qi, L. Wang, Z. Li, J. Sun, and J. Jia, "Fully Convolutional Networks for Panoptic Segmentation," in *Proceedings of the IEEE Conference on Computer Vision and Pattern Recognition (CVPR)*, 2021, pp. 214–223.
- [7] A. Hermans, L. Beyer, and B. Leibe, "In Defense of the Triplet Loss for Person Re-Identification," *arXiv preprint arXiv:1703.07737*, 2017.
- [8] W. Ye, H. Li, T. Zhang, X. Zhou, H. Bao, and G. Zhang, "SuperPlane: 3D Plane Detection and Description from a Single Image," in *2021 IEEE Virtual Reality and 3D User Interfaces (VR)*, 2021, pp. 207–215.
- [9] Z. Teed and J. Deng, "RAFT: Recurrent All-Pairs Field Transforms for Optical Flow," in *Proceedings of the European Conference on Computer Vision (ECCV)*. Springer, 2020, pp. 402–419.
- [10] W. Wang, T. Zhou, F. Porikli, D. Crandall, and L. Van Gool, "A Survey on Deep Learning Technique for Video Segmentation," *arXiv preprint arXiv:2107.01153*, 2021.
- [11] J. Li, W. Wang, J. Chen, L. Niu, J. Si, C. Qian, and L. Zhang, "Video Semantic Segmentation via Sparse Temporal Transformer," in *Proceedings of the 29th ACM International Conference on Multimedia (ACM MM)*, 2021, pp. 59–68.
- [12] L. Hoyer, D. Dai, Y. Chen, A. Koring, S. Saha, and L. Van Gool, "Three Ways to Improve Semantic Segmentation with Self-Supervised Depth Estimation," in *Proceedings of the IEEE/CVF Conference on Computer Vision and Pattern Recognition (CVPR)*, 2021, pp. 11 130–11 140.
- [13] L.-C. Chen, R. G. Lopes, B. Cheng, M. D. Collins, E. D. Cubuk, B. Zoph, H. Adam, and J. Shlens, "Naive-Student: Leveraging Semi-Supervised Learning in Video Sequences for Urban Scene Segmentation," in *Proceedings of the European Conference on Computer Vision (ECCV)*. Springer, 2020, pp. 695–714.
- [14] Y. Liu, C. Shen, C. Yu, and J. Wang, "Efficient Semantic Video Segmentation with Per-frame Inference," in *Proceedings of the European Conference on Computer Vision (ECCV)*. Springer, 2020, pp. 352–368.
- [15] Z. Yin, J. Zheng, W. Luo, S. Qian, H. Zhang, and S. Gao, "Learning to Recommend Frame for Interactive Video Object Segmentation in the Wild," in *Proceedings of the IEEE/CVF Conference on Computer Vision and Pattern Recognition (CVPR)*, 2021, pp. 15 445–15 454.
- [16] Y. Heo, Y. J. Koh, and C.-S. Kim, "Guided Interactive Video Object Segmentation Using Reliability-Based Attention Maps," in *Proceedings of the IEEE/CVF Conference on Computer Vision and Pattern Recognition (CVPR)*, 2021, pp. 7322–7330.
- [17] H. K. Cheng, Y.-W. Tai, and C.-K. Tang, "Modular Interactive Video Object Segmentation: Interaction-to-Mask, Propagation and Difference-Aware Fusion," in *Proceedings of the IEEE/CVF Conference on Computer Vision and Pattern Recognition (CVPR)*, 2021, pp. 5559–5568.
- [18] Z. Xu, W. Zhang, X. Tan, W. Yang, H. Huang, S. Wen, E. Ding, and L. Huang, "Segment as Points for Efficient Online Multi-Object Tracking and Segmentation," in *Proceedings of the European Conference on Computer Vision (ECCV)*. Springer, 2020, pp. 264–281.
- [19] Y. Li, N. Xu, J. Peng, J. See, and W. Lin, "Delving into the Cyclic Mechanism in Semi-supervised Video Object Segmentation," *Advances in Neural Information Processing Systems (NeurIPS)*, vol. 33, pp. 1218–1228, 2020.
- [20] H. Xie, H. Yao, S. Zhou, S. Zhang, and W. Sun, "Efficient Regional Memory Network for Video Object Segmentation," in *Proceedings of the IEEE/CVF Conference on Computer Vision and Pattern Recognition (CVPR)*, 2021, pp. 1286–1295.
- [21] B. Duke, A. Ahmed, C. Wolf, P. Aarabi, and G. W. Taylor, "SSTVOS: Sparse Spatiotemporal Transformers for Video Object Segmentation," in *Proceedings of the IEEE/CVF Conference on Computer Vision and Pattern Recognition (CVPR)*, 2021, pp. 5912–5921.
- [22] S. Ren, W. Liu, Y. Liu, H. Chen, G. Han, and S. He, "Reciprocal Transformations for Unsupervised Video Object Segmentation," in *Proceedings of the IEEE/CVF Conference on Computer Vision and Pattern Recognition (CVPR)*, 2021, pp. 15 455–15 464.
- [23] L. Porzi, M. Hofinger, I. Ruiz, J. Serrat, S. R. Bulo, and P. Kotschieder, "Learning Multi-Object Tracking and Segmentation from Automatic Annotations," in *Proceedings of the IEEE/CVF Conference on Computer Vision and Pattern Recognition (CVPR)*, 2020, pp. 6846–6855.
- [24] J. Luiten, I. E. Zulfikar, and B. Leibe, "UnOVOST: Unsupervised Offline Video Object Segmentation and Tracking," in *Proceedings of the IEEE/CVF Winter Conference on Applications of Computer Vision (WACV)*, 2020, pp. 2000–2009.
- [25] Y. Yang, B. Lai, and S. Soatto, "DyStaB: Unsupervised Object Segmentation via Dynamic-Static Bootstrapping," in *Proceedings of the IEEE/CVF Conference on Computer Vision and Pattern Recognition (CVPR)*, 2021, pp. 2826–2836.
- [26] T. Hui, S. Huang, S. Liu, Z. Ding, G. Li, W. Wang, J. Han, and F. Wang, "Collaborative Spatial-Temporal Modeling for Language-Queried Video Actor Segmentation," in *Proceedings of the IEEE/CVF Conference on Computer Vision and Pattern Recognition (CVPR)*, 2021, pp. 4187–4196.
- [27] L. Ye, M. Rochan, Z. Liu, X. Zhang, and Y. Wang, "Referring Segmentation in Images and Videos with Cross-Modal Self-Attention Network," *arXiv preprint arXiv:2102.04762*, 2021.
- [28] B. McIntosh, K. Duarte, Y. S. Rawat, and M. Shah, "Visual-Textual Capsule Routing for Text-Based Video Segmentation," in *Proceedings of the IEEE/CVF Conference on Computer Vision and Pattern Recognition (CVPR)*, 2020, pp. 9942–9951.
- [29] T. Zhou, J. Li, X. Li, and L. Shao, "Target-aware object discovery and association for unsupervised video multi-object segmentation," in *Proceedings of the IEEE/CVF Conference on Computer Vision and Pattern Recognition (CVPR)*, 2021, pp. 6985–6994.

- [30] C. Ventura, M. Bellver, A. Girbau, A. Salvador, F. Marques, and X. Giro-i Nieto, "RVOS: End-to-End Recurrent Network for Video Object Segmentation," in *Proceedings of the IEEE/CVF Conference on Computer Vision and Pattern Recognition (CVPR)*, 2019, pp. 5277–5286.
- [31] Y. Wang, Z. Xu, X. Wang, C. Shen, B. Cheng, H. Shen, and H. Xia, "End-to-End Video Instance Segmentation with Transformers," in *Proceedings of the IEEE/CVF Conference on Computer Vision and Pattern Recognition (CVPR)*, 2021.
- [32] A. Athar, S. Mahadevan, A. Osep, L. Leal-Taixé, and B. Leibe, "STEm-Seg: Spatio-temporal Embeddings for Instance Segmentation in Videos," in *Proceedings of the European Conference on Computer Vision (ECCV)*. Springer, 2020, pp. 158–177.
- [33] G. Bertasius and L. Torresani, "Classifying, Segmenting, and Tracking Object Instances in Video with Mask Propagation," in *Proceedings of the IEEE/CVF Conference on Computer Vision and Pattern Recognition (CVPR)*, 2020, pp. 9739–9748.
- [34] J. Cao, R. M. Anwer, H. Cholakkal, F. S. Khan, Y. Pang, and L. Shao, "SipMask: Spatial Information Preservation for Fast Image and Video Instance Segmentation," in *Proceedings of the European Conference on Computer Vision (ECCV)*, 2020.
- [35] X. Ying, X. Li, and M. C. Chuah, "SRNet: Spatial Relation Network for Efficient Single-stage Instance Segmentation in Videos," in *Proceedings of the 29th ACM International Conference on Multimedia (ACM MM)*, 2021, pp. 347–356.
- [36] H. Lin, R. Wu, S. Liu, J. Lu, and J. Jia, "Video Instance Segmentation with a Propose-Reduce Paradigm," in *Proceedings of the IEEE/CVF International Conference on Computer Vision (ICCV)*, 2021, pp. 1739–1748.
- [37] S. Qiao, Y. Zhu, H. Adam, A. Yuille, and L.-C. Chen, "ViP-DeepLab: Learning Visual Perception with Depth-aware Video Panoptic Segmentation," in *Proceedings of the IEEE/CVF Conference on Computer Vision and Pattern Recognition (CVPR)*, 2021, pp. 3997–4008.
- [38] M. Weber, J. Xie, M. Collins, Y. Zhu, P. Voigtlaender, H. Adam, B. Green, A. Geiger, B. Leibe, D. Cremers, A. Osep, L. Leal-Taixé, and L.-C. Chen, "STEP: Segmenting and Tracking Every Pixel," in *Neural Information Processing Systems (NeurIPS) Track on Datasets and Benchmarks*, 2021.
- [39] Y. Zhang, C. Wang, X. Wang, W. Zeng, and W. Liu, "FairMOT: On the Fairness of Detection and Re-Identification in Multiple Object Tracking," *arXiv preprint arXiv:2004.01888*, 2020.
- [40] J. Pang, L. Qiu, X. Li, H. Chen, Q. Li, T. Darrell, and F. Yu, "Quasi-Dense Similarity Learning for Multiple Object Tracking," in *Proceedings of the IEEE/CVF Conference on Computer Vision and Pattern Recognition (CVPR)*, June 2021, pp. 164–173.
- [41] Z. Wang, L. Zheng, Y. Liu, and S. Wang, "Towards Real-Time Multi-Object Tracking," *arXiv preprint arXiv:1909.12605*, 2019.
- [42] K. He, G. Gkioxari, P. Dollar, and R. Girshick, "Mask R-CNN," in *Proceedings of the IEEE International Conference on Computer Vision (ICCV)*, Oct 2017.
- [43] F. Milletari, N. Navab, and S.-A. Ahmadi, "V-Net: Fully Convolutional Neural Networks for Volumetric Medical Image Segmentation," in *Proceedings of the International Conference on 3D Vision (3DV)*. IEEE, 2016, pp. 565–571.
- [44] T.-Y. Lin, P. Goyal, R. Girshick, K. He, and P. Dollár, "Focal Loss for Dense Object Detection," 2018.
- [45] H. Yu, W. Ye, Y. Feng, H. Bao, and G. Zhang, "Learning Bipartite Graph Matching for Robust Visual Localization," in *2020 IEEE International Symposium on Mixed and Augmented Reality (ISMAR)*. IEEE, 2020, pp. 146–155.
- [46] Q. Wang, X. Zhou, B. Hariharan, and N. Snavely, "Learning Feature Descriptors using Camera Pose Supervision," in *Proceedings of the European Conference on Computer Vision (ECCV)*, 2020.
- [47] X. Wang, A. Jabri, and A. A. Efros, "Learning Correspondence from the Cycle-Consistency of Time," in *Proceedings of the IEEE/CVF Conference on Computer Vision and Pattern Recognition (CVPR)*, 2019.